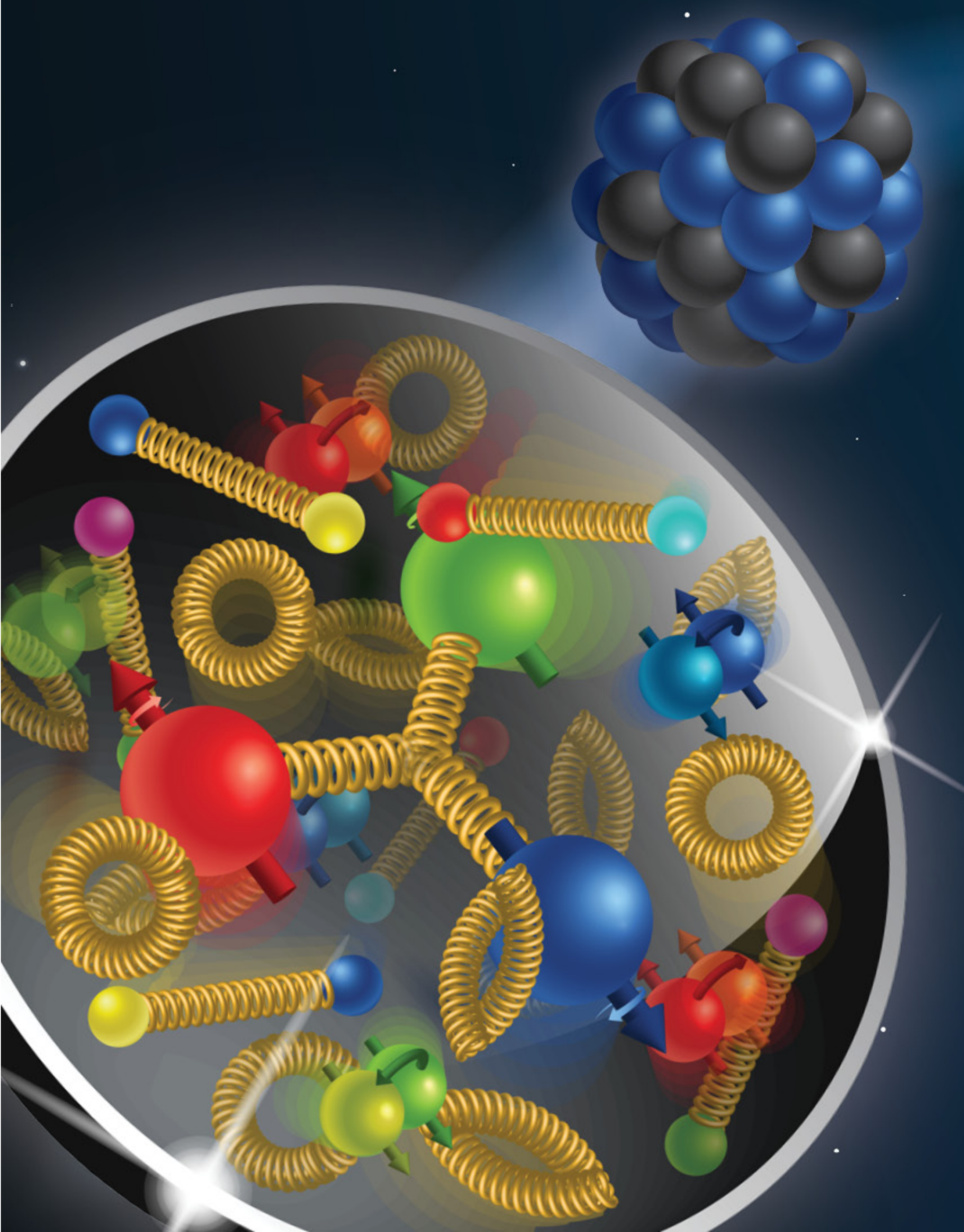

Combined Effect of IBS and Impedance on the Longitudinal Beam Dynamics

Oct. 29, 2020

Alexei Blednykh, BNL/EIC

8th Low Emittance Rings Workshop
INFN-LNF, Frascati, 26-30 October 2020

Electron-Ion Collider

Outlook

- **NSLS-II main parameters**
- **NSLS-II Longitudinal Impedance Budget**
- **Diagnostic Methods**
- **Microwave Instability Threshold & Beam Pattern**
- **Combined Effect of IBS and Wakefield**

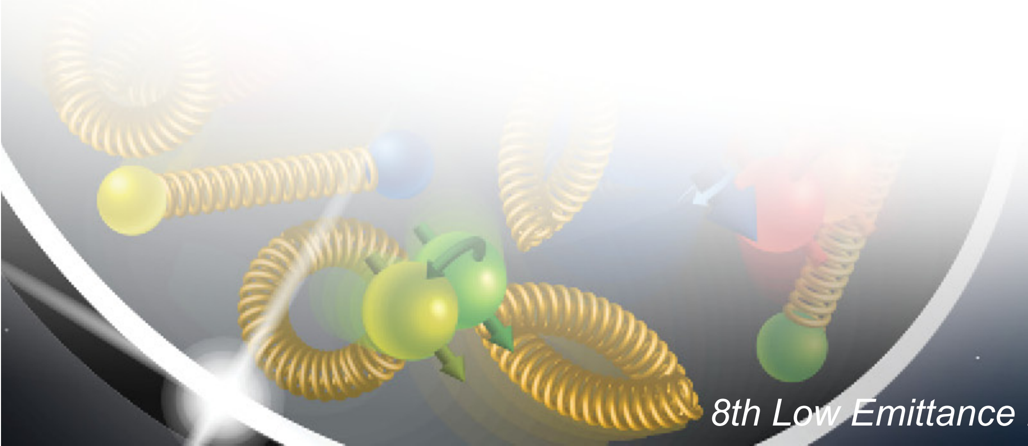

NSLS-II Achieves Design Beam Current 500mA!

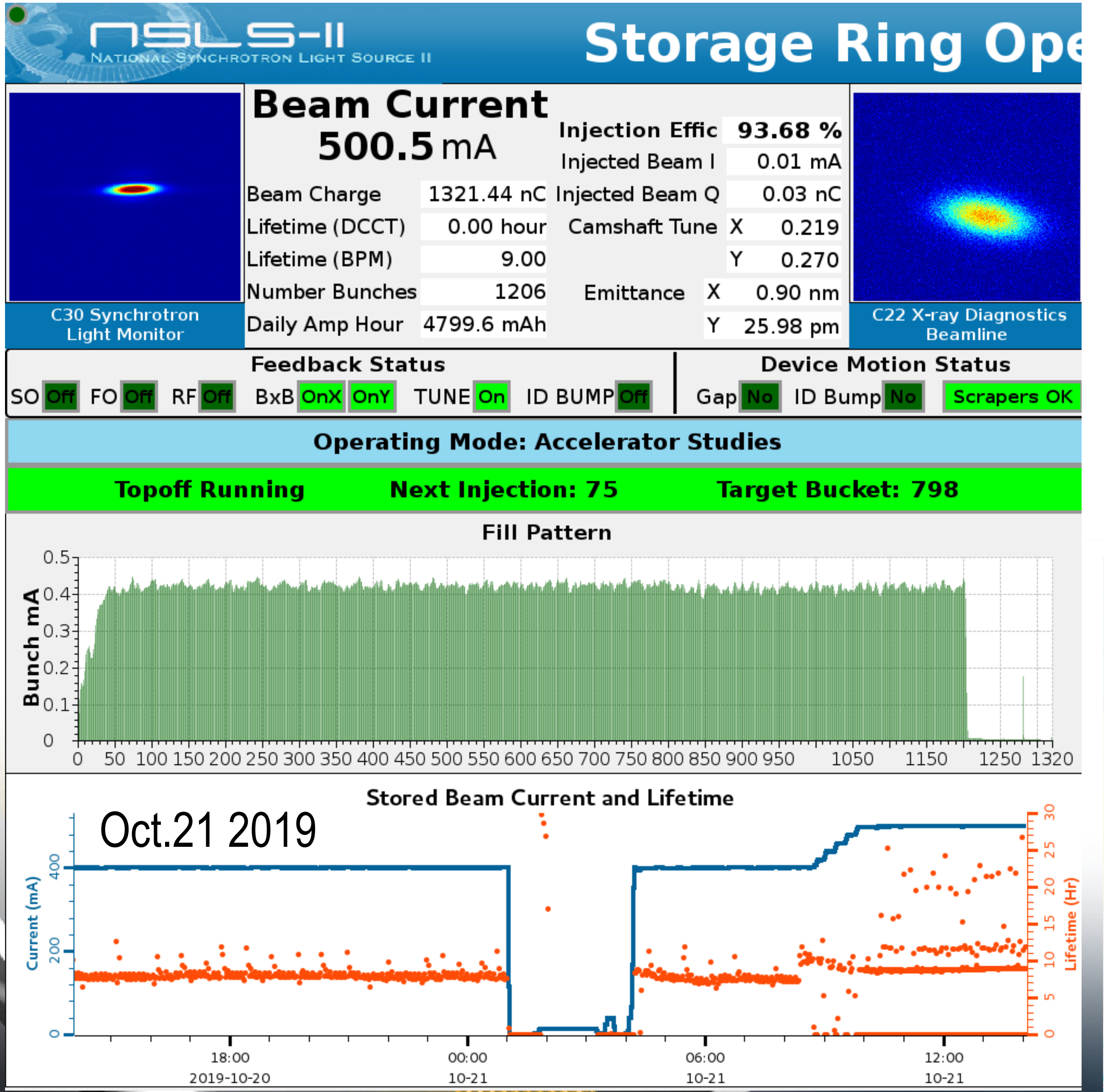

NSLS-II NATIONAL SYNCHROTRON LIGHT SOURCE II

Storage Ring Ope

Beam Current
500.5 mA

Beam Charge	1321.44 nC	Injection Effic		93.68 %
Lifetime (DCCT)	0.00 hour	Injected Beam I		0.01 mA
Lifetime (BPM)	9.00	Injected Beam Q		0.03 nC
Number Bunches	1206	Camshaft Tune	X	0.219
Daily Amp Hour	4799.6 mAh		Y	0.270
		Emittance	X	0.90 nm
			Y	25.98 pm

C30 Synchrotron Light Monitor

C22 X-ray Diagnostics Beamline

Feedback Status

SO Off FO Off RF Off BxB OnX OnY TUNE On ID BUMP Off

Device Motion Status

Gap No ID Bump No Scrapers OK

Operating Mode: Accelerator Studies

Topoff Running **Next Injection: 75** **Target Bucket: 798**

Fill Pattern

Stored Beam Current and Lifetime

Oct.21 2019

- We invested into creating diagnostic and monitoring devices since we had concern about the localized heating of the vacuum components, Bellows, RF Contact Spring, Septum Chamber, Stripline Kicker, Ceramics Chambers.
- IR thermal view cameras and temperature sensors available around the ring for temperature monitoring
- Available diagnostic helped us in fixing problems and reaching 500 mA.
- The beam is stable at chromaticity +2/+2 with Transverse Feedback System “ON”. A 10% gap for ion clearing.

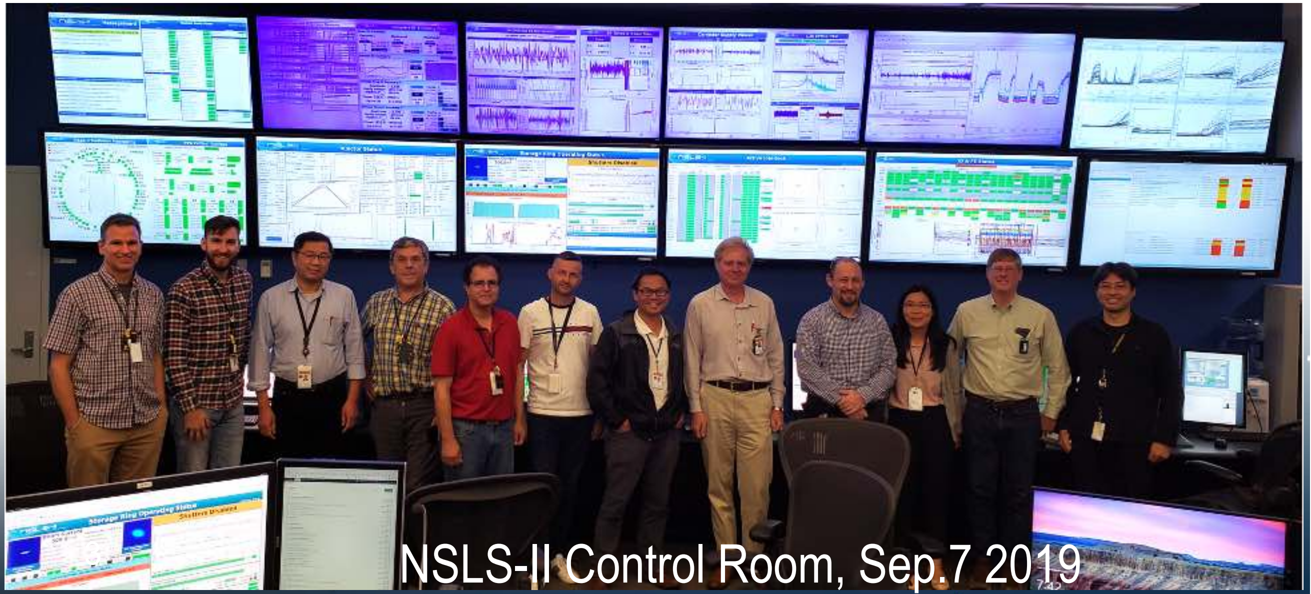

NSLS-II Control Room, Sep.7 2019

Main NSLS-II Parameters

Energy	$E_0 (GeV)$	3		
Revolution period	$T_0 (\mu s)$	2.6		
Momentum compaction	α	3.7 x 10^{-4}		
RF voltage	$V_{RF} (MV)$	3.4 (One RF system)		
Synchrotron tune	ν_s	9.2 x 10^{-3}		
		BL	1DW	3DW
Energy loss	$U (keV)$	287	400	674
Damping time	$\tau_x, \tau_s \ (ms)$	54, 27	40, 20	23, 11.5
Energy spread	σ_δ	0.5 x 10^{-3}	0.71 x 10^{-3}	0.82 x 10^{-3}
Horizontal Emittance	$\varepsilon_x \ (nm)$	2.1	1.4	0.9
Bunch length (at low current)	$\sigma_z \ (mm)$	2.5	3.5	4

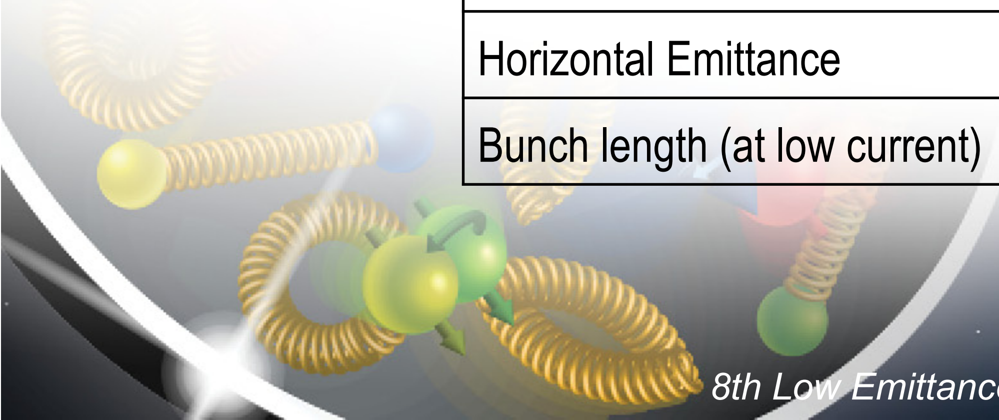

NSLS-II Longitudinal Impedance Budget

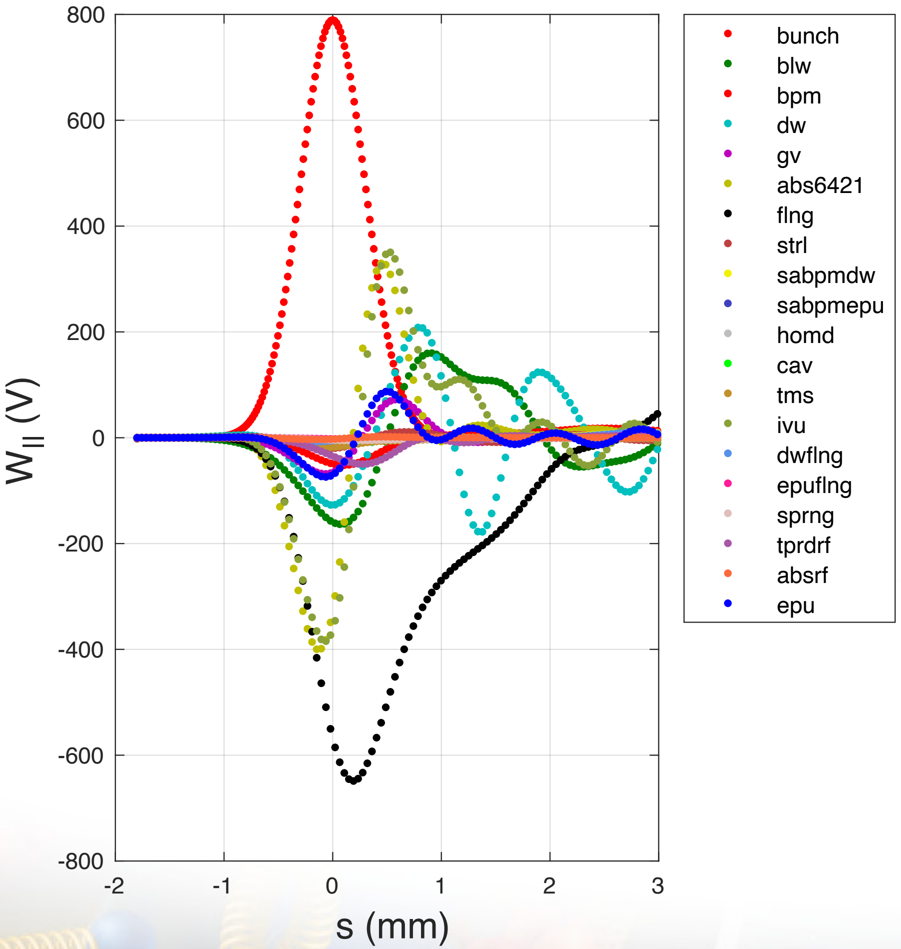

The longitudinal short-range wakepotential for each individual component (multiplied by the number of the components)

		Number of components
Bellows	BLW	218
Large Aperture BPM	LABPM	237
Small Aperture BPM (11.5mm x 60mm)	SABPMDW	10
Small Aperture BPM (8mm x 55mm)	SABPMEPU	3
Damping Wiggler Chamber (11.5mm x 60mm)	DW	3
Elliptically Polarized Undulator Chamber (11.5mm x 60mm)	EPU1	2
Elliptically Polarized Undulator Chamber (8mm x 55mm)	EPU2	2
Gate Valve (Standard)	GV	61
Flange Absorber (21mm x 64mm)	FABS	67
Flange Absorber S4 (21mm x 64mm)	FABSS4	39
Flange Absorber Rest – not included	FABS2	7
Stripline (BBF), L=300mm	SL300	2
Standard RF Sealed Flanges	FLNG	739
EPU RF Sealed Flanges	EPUFLNG	4
DW RF Sealed Flanges	DWFLNG	13
Direct-Current Current Transformer – not included	DCCT	1
Kickers Ti-Coated Ceramics Chambers	CCHM	5
RF HOM Damper	HOMD	2
500 MHz RF Cavity*	CAV	2
RF Tapered Transition	TPRDRF	1
RF Flange Absorber (21mm x 64mm)	FABSRF	1
Stripline (TMS), L=150mm	SL150	2
In-Vacuum Undulator	IVU	9

NSLS-II Total Longitudinal Wakefield

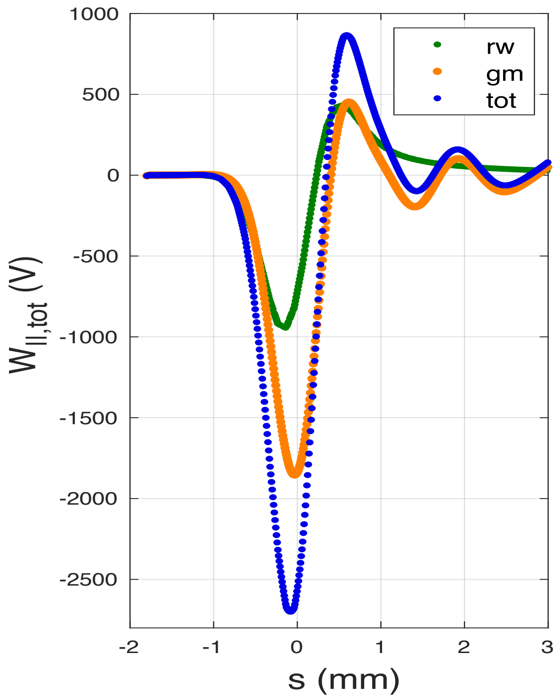

Total longitudinal wakepotential of NSLS-II

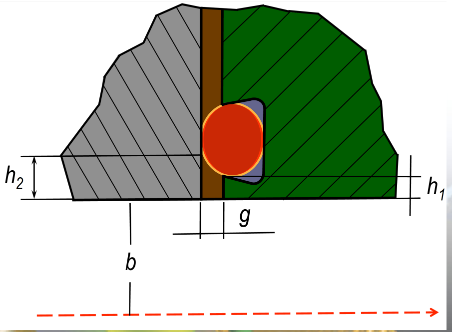

Details of the flange joint

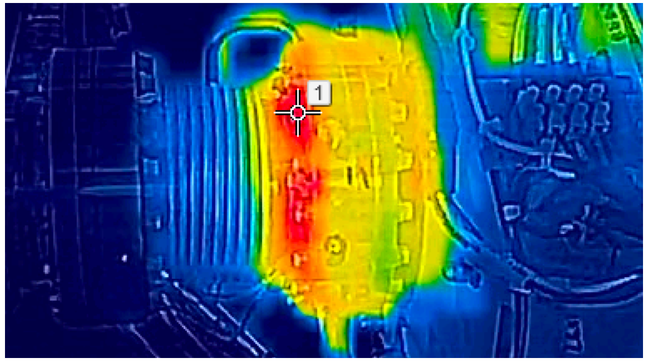

IR thermal image of the the flange joints

RF spring in a special groove

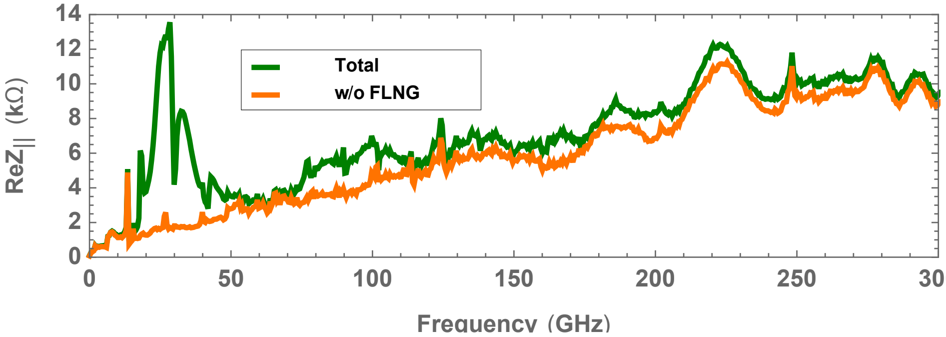

Real part of the longitudinal impedance

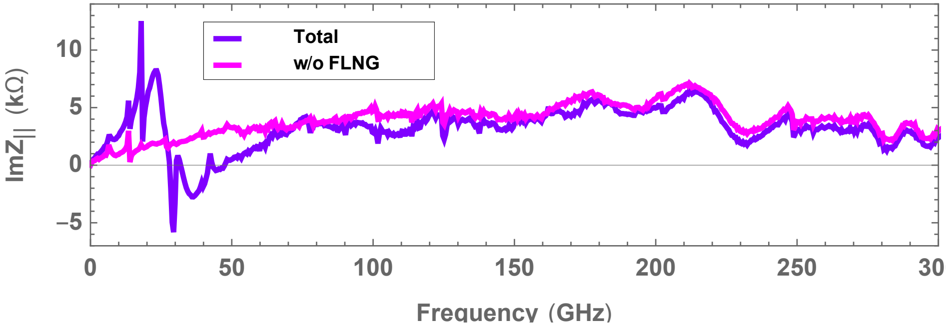

Imaginary part of the longitudinal impedance

- RW + GdfidL simulated geometric (gm) wakefields for a 0.3mm bunch length.
- Limitation on the single-bunch current result from ~740 RF contact springs design.
- Beam is stable at 500mA within M=1050 bunches (0.5mA/bunch)

Electron Beam Diagnostic Methods

- In-Vacuum Undulator Radiation Spectrum
- Synchrotron Light Monitor Camera ($\eta_x = 0.13\mathrm{m}$)
- Pinhole Camera (zero dispersion)
- Beam Spectra Spectra Measurements
  - BPM & Stripline Kickers - Network Analyzer
  - Infra-Red Optical Extraction Beamline (Large Aperture Dipole Chamber) - THz Schottky-diode detector

- O. Chubar, C. Kitegi, Y. Chen-Wiegart, D. Hidas, Y. Hidaka, T. Tanabe, G. Williams, J. Thieme, T. Caswell, M. Rakitin, L. Wiegart, A. Fluerasu, L. Yang, S. Chodankar, M. Zhernenkov, “Spectrum-Based Alignment of In-Vacuum Undulators in a Low-Emittance Storage Ring”, Synchrotron Radiation News, Vol.31, No.3, pp.4-8 (2018).

- W. Anders, Proceedings of EPAC1992, Berlin, Germany, 24-28 March 1992. Miriam Brosi and etc., Phys. Rev. Accel. Beams 22, 020701 – Published 13 February 2019.

- W. Anders, Proceedings of EPAC1992, Berlin, Germany, 24-28 March 1992.

- Y.-C. Chae, L. Emery, A.H. Lumpkin, J. Song, B.X. Yang, Proceedings of the 2001 Particle Accelerator Conference, Chicago, 2001.

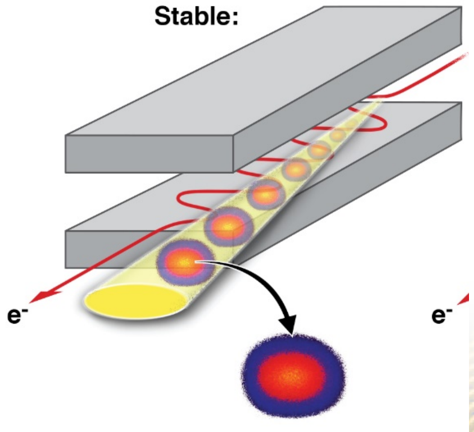

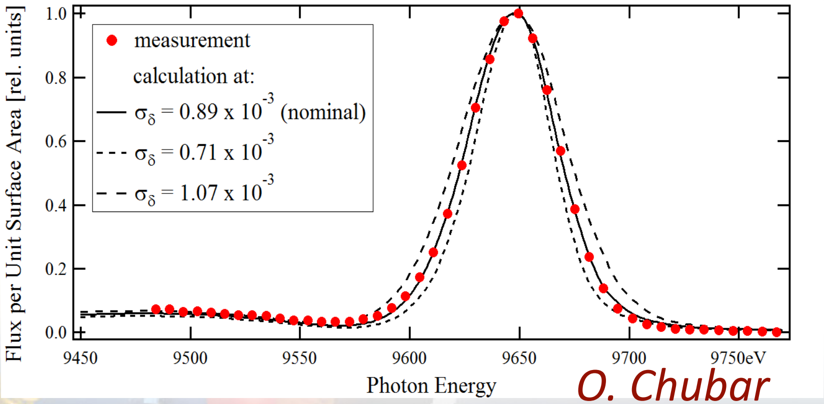

O. Chubar

On axis UR spectrum measured at 7th harmonic of the IVU20 at the CHX NSLS-II beamline

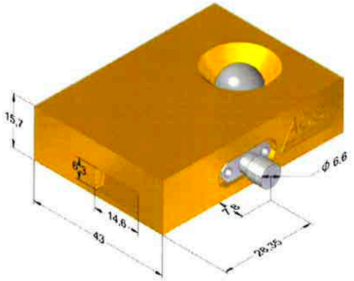

22-IR UHV Optical Extraction Beamline

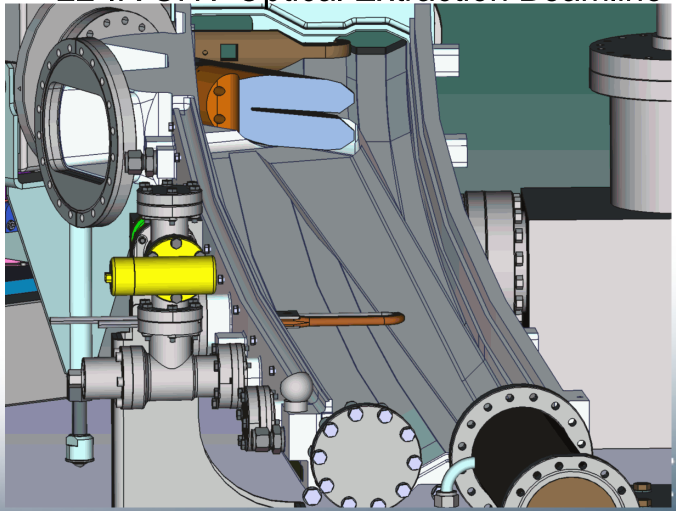

Energy Spread Dependence on the Lattice

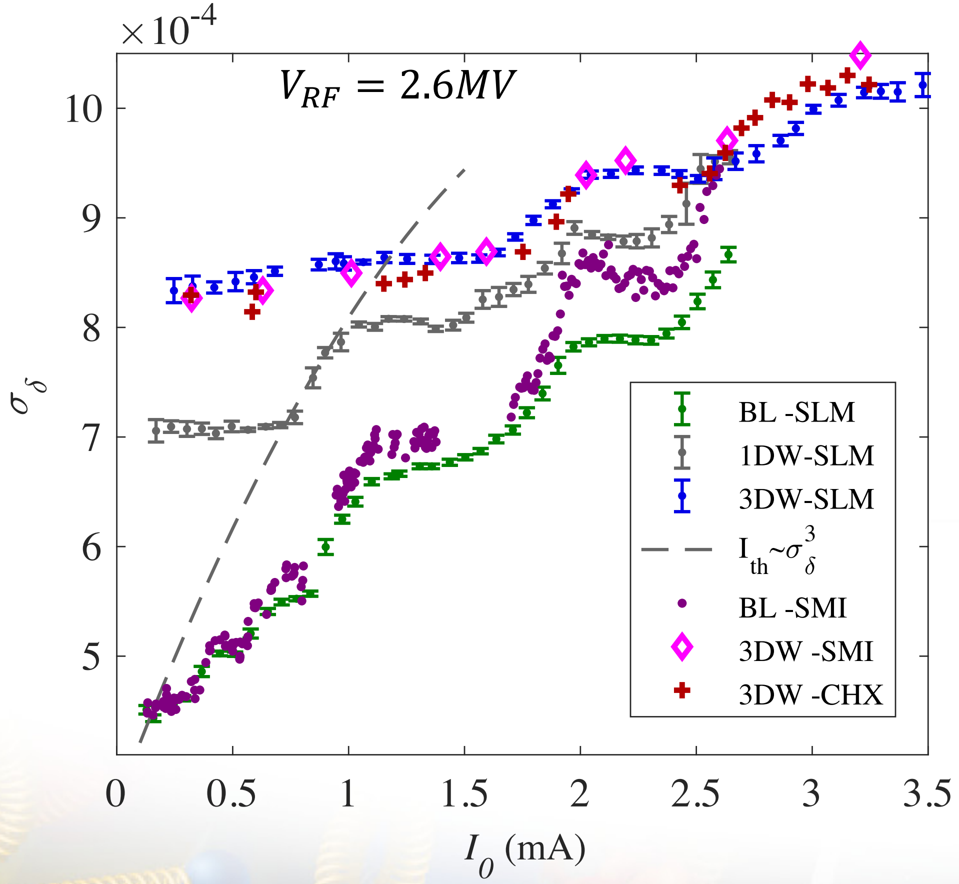

- The energy spread data estimated from IVU's spectral measurements are shown for BL with purple dots, 3DW with magenta diamonds (SMI beamline) and 3DW with wine crosses (CHX beamline)
- The dependence of the microwave instability threshold on the energy spread according to the scaling law $\mathrm{I_{th1}} \sim \alpha\sigma_\delta^3$ is shown with the dashed grey line.
- The SLM camera data are presented for three different lattices, BL (green trace), 1DW (grey trace) and 3DW (blue trace) at $V_{RF} = 2.6MV$. The energy spread is derived from the horizontal beam size measurements $\sigma_x(I_0)$.

$$\sigma_\delta(I_0) = \frac{1}{\eta_x}\sqrt{\sigma_x^2(I_0) - \varepsilon_x(I_0)\beta_x} \qquad \text{Eq. (1)}$$

With $\sigma_x = 123\mathrm{um}$, $\beta_x = 2.77\mathrm{m}$, $\eta_x = 0.13\mathrm{m}$ and $\varepsilon_x = 0.9\mathrm{nm}$ for the 3DW - $\sigma_\delta = 0.087\%$

Microwave Fill-Pattern Measurements

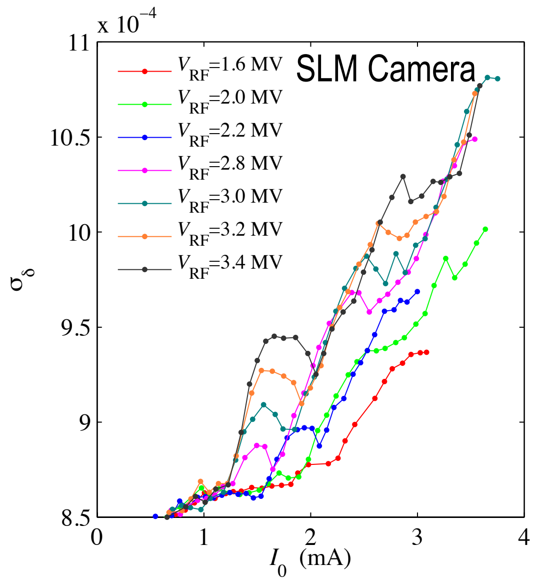

Energy spread dependence vs. single-bunch current

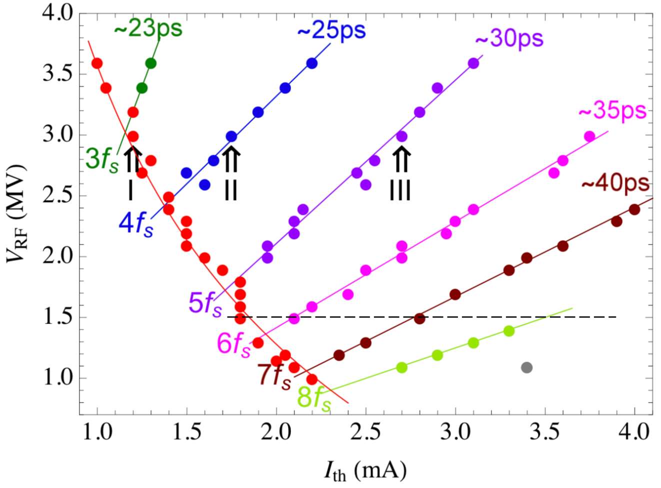

The instability threshold currents at different V_{RF}

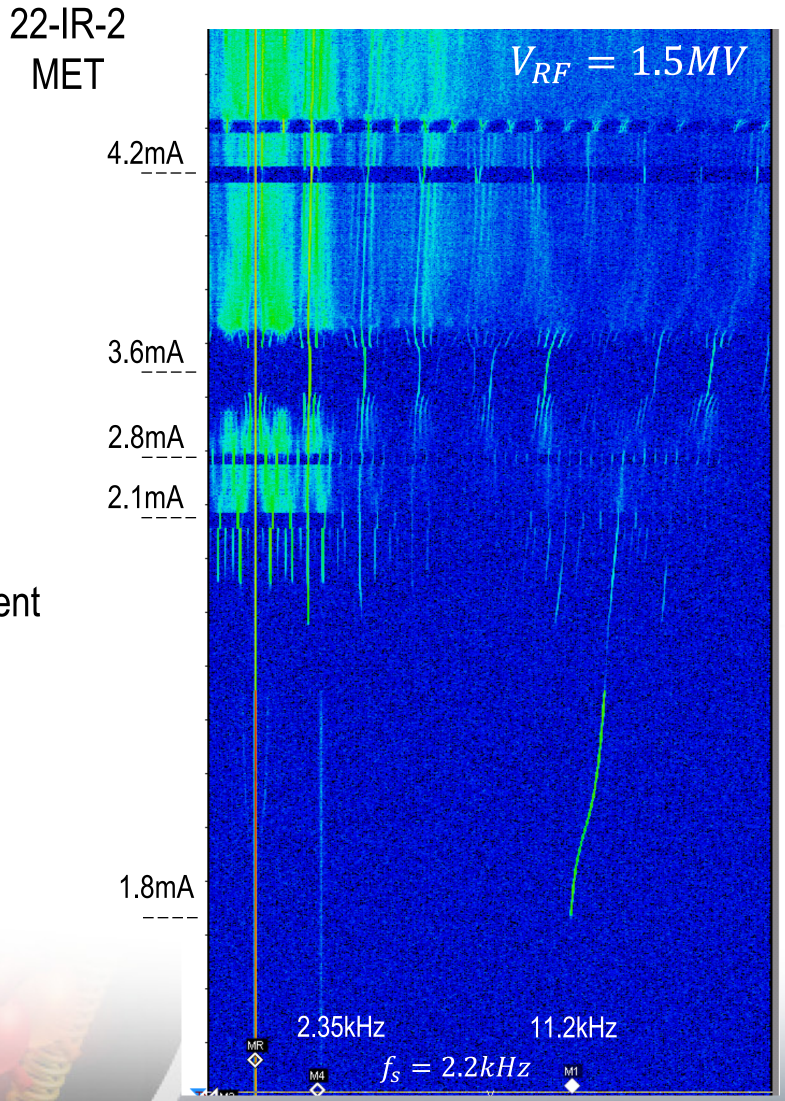

- Beam spectra at $V_{RF} = 1.5MV$
- 3DW Lattice
- The local minima of the energy spread as a certain threshold current I_{th} where two initially distinct frequencies merge, which we interpret as classical mode coupling as first described by Sacherer.
- However we were not able to observe, experimentally and numerically, the oscillating frequencies of the longitudinal modes before the beam becomes unstable

- A. Blednykh, B. Bacha, G. Bassi, W. Cheng, O. Chubar, A. Derbenev, R. Lindberg, M. Rakitin, V. Smaluk, M. Zhernenkov, Yu-chen Karen Chen-Wiegart and L. Wiegart, "New aspects of longitudinal instabilities in electron storage rings", Scientific Reports volume 8, Article number: 11918 (2018).

Energy Spread and Bunch Length Dependence

Experimental Data

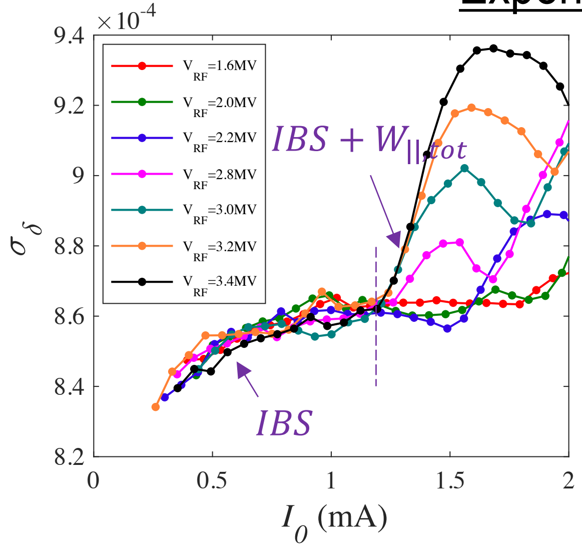

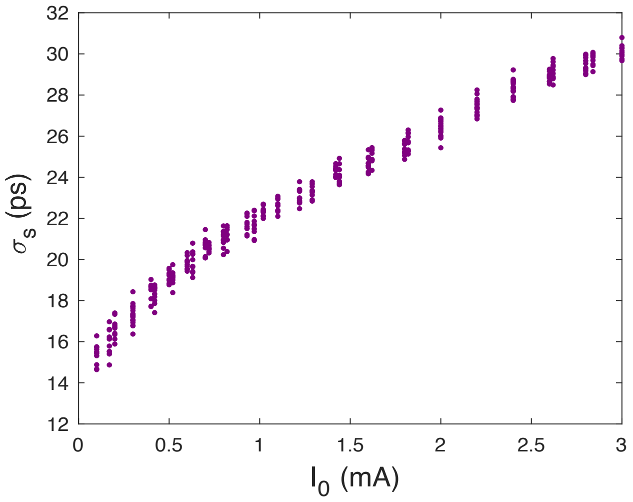

Numerically Simulated Data

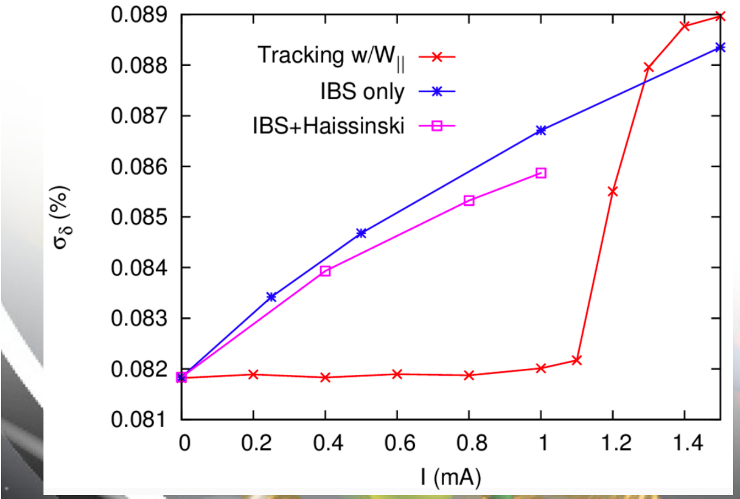

Energy spread vs. single-bunch current

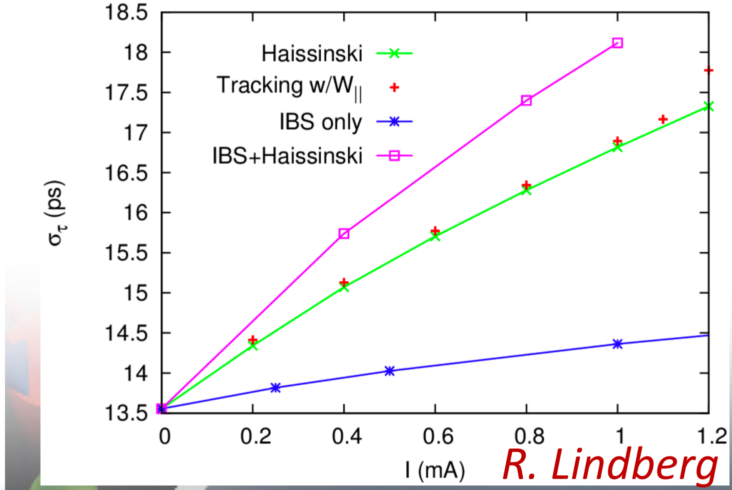

R. Lindberg

Bunch length vs. single-bunch current

- Energy spread (σ_δ) growth below the microwave instability threshold (I_{th}) can be explained by the Intra-Beam Scattering (IBS) effect
- Microwave beam pattern is due to the total longitudinal wakefield ($W_{||,tot}$)
- Bunch length measured by the streak camera.
- Tracking with $W_{||,tot}$ only shows σ_δ remains unchanged at $I_0 < I_{th}$.
- Energy spread and bunch length increase resulting from the IBS effect has been estimated by the ibsemittance code.
- IBS + Wakefield need to be simulated simultaneously!

Combined Effect of IBS & Wakefield

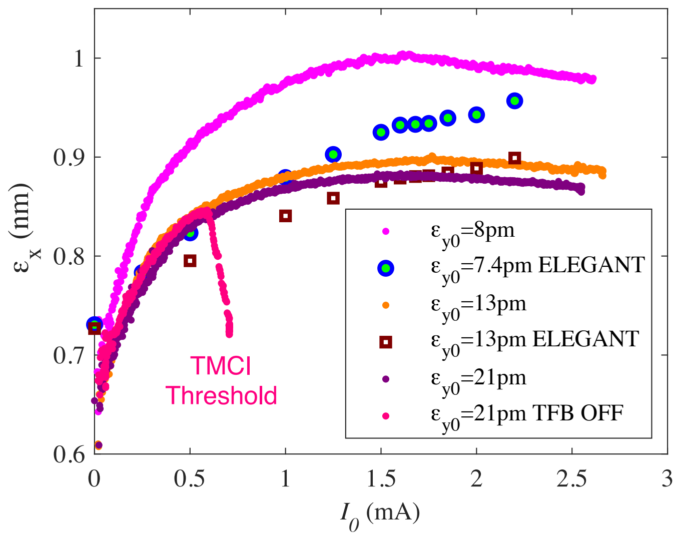

Horizontal emittance vs. single bunch current

- V. Smaluk et al. PHYS. REV. ACCEL. BEAMS 22, 124001 (2019)

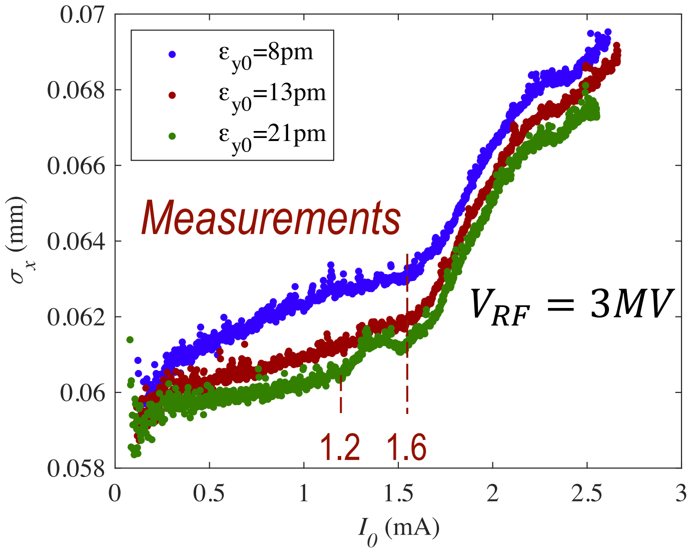

Horizontal beam size vs. single-bunch current

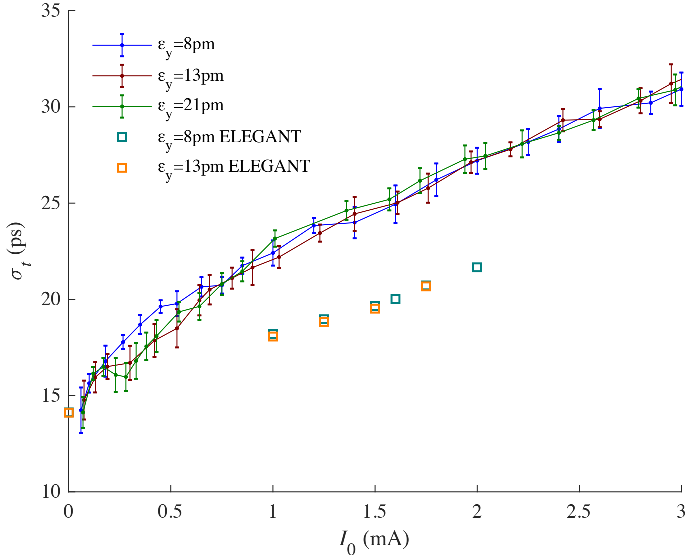

Bunch length vs. single-bunch current

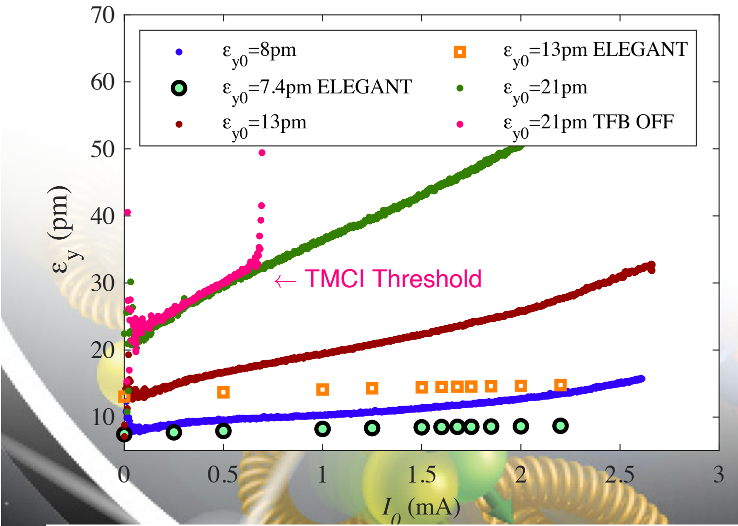

Vertical emittance vs. single bunch current

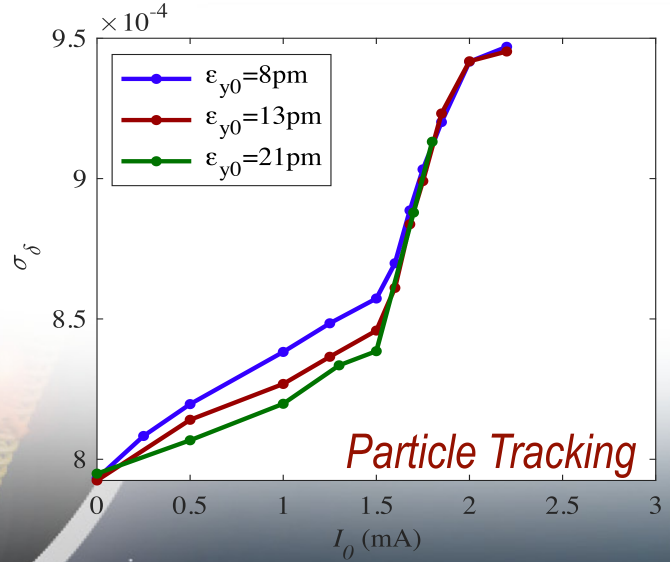

ELEGANT simulations of $\sigma_\delta(I_0)$ dependence

- The IBS effect results in increase the microwave instability threshold ($I_{th,\mu w}$) .
- ELEGANT simulations with 160+ cores using the element-by-element NSLS-II lattice.
- Significant emittance growth vs. I_0
- TMCI threshold is 0.7mA at chromaticity +2/+2
- The same trend of $\varepsilon_y(I_0)$ growth with and w/o BBFS below the TMCI threshold

Electron-Ion Collider

Vertical Emittance Growth

- If ε_y - growth is a cause of the betatron coupling (zero vertical dispersion), then:

$$\frac{\varepsilon_y}{\varepsilon_{y0}} = \frac{\varepsilon_x}{\varepsilon_{x0}}$$

- K. Bane *et al*., in *Proceedings of the Particle Accelerator Conference, Chicago, IL, 2001* (IEEE, Piscataway, NJ, 2001), p. 2995.

- KUBO, MTINGWA, AND WOLSKI, Phys. Rev. ST Accel. Beams **8,** 081001 (2005)

- ε_y - growth at $I_0 < 1mA$ is due to the bettatron coupling.
- ε_y - growth at $I_0 > 1mA$ needs to be further investigated.
- Stabilizing effect of the Transverse Bunch-by-Bunch Feed Back System (BBFS) on the single bunch current. $I_0 > 6mA$ with BBFS "On". Does it effect ε_y at $I_0 > 1mA$?
- Adjusting the strength of the skew quadrupole to increase the vertical emittance w/o further lattice correction.
- The ratio is not holding for 2% and 3% (vertical dispersion?)
- Insufficient diagnostic resolution at low current.

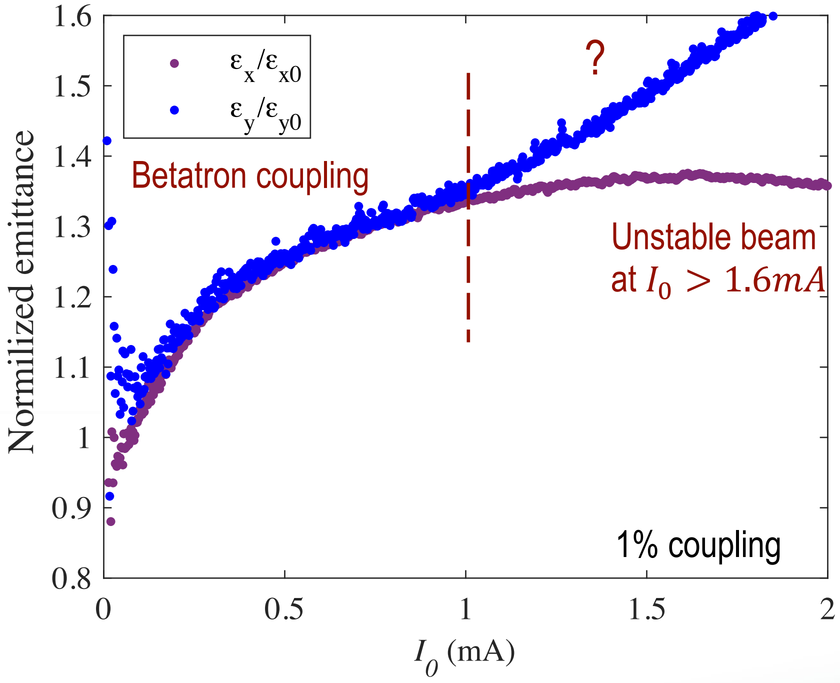

Experimental results of the normalized emittance for 1% coupling

Summary

- We have found and cross-checked changes in the electron beam energy spread at NSLS-II.
- Monotonic energy spread growth, below the microwave instability threshold, is due to the IBS effect .
- We benchmarked the ELEGANT code using the combined effect of IBS and $W_{||,tot}$ vs. the experimental data. Particle tracking simulations confirm the IBS effect on the microwave instability threshold.
- The IBS effect result in increase of $\sigma_s(I_0)$ and $\sigma_\delta(I_0)$.
- All diagnostic methods require the tune-up procedures to perform the precise measurements. Beam lines and the pinhole cameras need to be recalibrated before each beam study shift.

Acknowledgments

- **BNL/NSLS-II**

  G. Bassi, B. Bacha, T. Shaftan, V. Smaluk, A. Derbenev, O. Chubar, M. Zhernenkov, L. Wiegart.

- **ANL/APS-U**

  R. Lindberg, M. Borland

- **LNF/INFN**

  M. Zobov